Current Biology, Vol. 14, 1515–1521, August 24, 2004, ©2004 Elsevier Ltd. All rights reserved. DOI 10.1016/j.cub.2004.08.033

Helical Growth of the *Arabidopsis* Mutant *tortifolia1* Reveals a Plant-Specific Microtubule-Associated Protein

Henrik Buschmann,[1,5] Christoph O. Fabri,[1] Monika Hauptmann,[1] Peter Hutzler,[2] Thomas Laux,[3] Clive W. Lloyd,[4] and Anton R. Schäffner[1,*]

[1]Institute of Biochemical Plant Pathology and
[2]Institute of Pathology
GSF – National Research Center for Environment and Health
D-85764 Neuherberg
Germany
[3]Institute of Biology III
University of Freiburg
D-79194 Freiburg
Germany
[4]Department of Cell and Developmental Biology
John Innes Centre
Colney, Norwich NR4 7UH
United Kingdom

Summary

Plants can grow straight or in the twisted fashion exhibited by the helical growth of some climbing plants. Analysis of helical-growth mutants from *Arabidopsis* has indicated that microtubules are involved in the expression of the helical phenotype. *Arabidopsis* mutants growing with a right-handed twist have been reported to have cortical microtubules that wind around the cell in left-handed helices and vice versa [1–3]. Microtubular involvement is further suspected from the finding that some helical mutants are caused by single amino acid substitutions in α-tubulin and because of the sensitivity of the growth pattern to anti-microtubule drugs. Insight into the roles of microtubules in organ elongation is anticipated from analyses of genes defined by helical mutations [4]. We investigated the helical growth of the *Arabidopsis* mutant *tortifolia1*/*spiral2* (*tor1*/*spr2*), which twists in a right-handed manner, and found that this correlates with a complex reorientation of cortical microtubules. *TOR1* was identified by a map-based approach; analysis of the TOR1 protein showed that it is a member of a novel family of plant-specific proteins containing N-terminal HEAT repeats. Recombinant TOR1 colocalizes with cortical microtubules in planta and binds directly to microtubules in vitro. This shows that TOR1 is a novel, plant-specific microtubule-associated protein (MAP) that regulates the orientation of cortical microtubules and the direction of organ growth.

Results and Discussion

During leaf expansion, *tortifolia1* (*tor1*) mutants show a striking twisting of leaf petioles, and this twisting results in a consistent right-handed displacement of the leaf blade [5]. This phenotype served as a template for screening an ethane methylsulfonate-generated mutant collection. We isolated left-handed and right-handed helical-growth mutants representing several complementation groups, but all *tor1* alleles showed right-handed organ twisting. Additional *tor1* alleles, including *spiral2* (*spr2*) [3], were obtained from other researchers and included in the investigation (see Table S1).

Analysis of petiole growth showed that the twisting phenotype of *tor1* is not expressed before the onset of cell elongation-driven organ growth (Figures S1A–S1E in the Supplemental Data available with this article online). Similarly, *tor1* hypocotyls were straight and indistinguishable from those of the wild-type in the early stages of organ growth (up to 4 days after germination [DAG]), but organ twisting became manifest during continued elongation growth; it started to appear at 5 DAG and was strongly expressed by 18 DAG (Figures 1A–1E). Because Gendreau et al. [6] have established that hypocotyl growth in *Arabidopsis* is almost exclusively based on cell elongation, this organ was chosen as more amenable material for the cell-biological analysis.

Drug studies and morphological analyses have been carried out for the *tor1*/*spr2* mutant [3], but no microtubule (MT) phenotype has been demonstrated. In the present paper the orientation of MTs in *tor1* hypocotyls was analyzed by immunofluorescence (Figures 1F–1I). During hypocotyl growth the angles of MTs beneath the outer epidermal walls were measured at 4 DAG, before the onset of twisting, and at 7 DAG, when twisting was apparent. Measurements were made relative to the long axis of the cell (Experimental Procedures). MTs perpendicular to that axis were categorized as transverse; values less than this had left-handed orientations, whereas larger values were classed as right handed. In the wild-type, it will be seen from Figure 1F that MT orientations of similar frequencies were spread over a broad range at 4 DAG (approximately from 50° to 130°), with MTs forming transverse as well as left-handed and right-handed helices. By 7 DAG this had evolved into a bimodal distribution, with more clearly resolved populations of left- and right-handed arrays (Figure 1H). This variability of array orientation is typical for aerial organs and has been reported for a variety of species [7–9]; it differs from the uniformity of the transverse MT arrays observed in the elongation zone of *Arabidopsis* roots [10, 11].

In comparison to those of wild-type hypocotyls, *tor1* MTs at 4 DAG show a remarkably sharper peak that indicates MTs to be more restricted to transverse and moderately oblique orientations (Figure 1G). By 7 DAG, most of the MT angles were less than 90°, showing that—in comparison to the equal split between left- and right-handed orientations seen in the wild-type—there was a pronounced bias toward left-handed arrays in *tor1* (Figure 1I). To provide a quantitative estimation of how MT orientations relate to the direction of cell elongation, we took mean values. At 4 DAG *tor1* and

*Correspondence: schaeffner@gsf.de
[5]Present address: Department of Cell and Developmental Biology, John Innes Centre, Colney, Norwich NR4 7UH, United Kingdom.

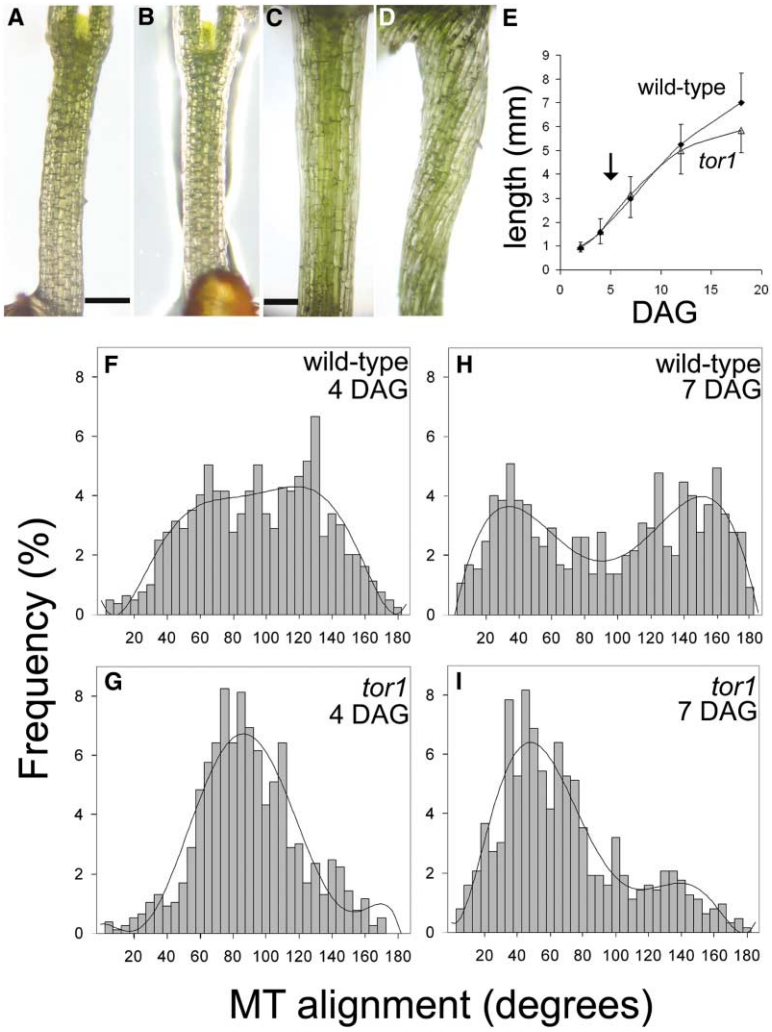

Figure 1. Growth of *Arabidopsis* Wild-Type and *tor1* Hypocotyls and Quantitative Analysis of MT Orientations

Plants were grown on soil with a 16/8 hr day/night cycle. At 4 DAG, hypocotyls are straight, but at 18 DAG *tor1* shows right-handed twisting of cell files.

(A) Wild-type, 4 DAG.

(B) *tor1*, 4 DAG.

(C) Wild-type, 18 DAG.

(D) *tor1*, 18 DAG.

(E) Growth curve for *Arabidopsis* wild-type and *tor1* hypocotyls. The arrow indicates the onset of helical growth at 5 DAG. (F–I) Quantitative analysis of MT orientations. Angles $<90°$ are left-handed MT orientations; angles $>90°$ are right-handed orientations.

(F) Wild-type, 4 DAG, mean MT orientation = 93.0°, SD = 38.3°.

(G) *tor1*, 4 DAG, mean MT orientation = 87.4°, SD = 30.2°.

(H) Wild-type, 7 DAG, mean MT orientation = 92.9°, SD = 52.1°.

(I) *tor1*, 7 DAG, mean MT orientation = 66.2°, SD = 38.6°. Trendlines were generated with Microsoft Excel. DAG days after germination. Scale bars in (A and B) and (C and D) represent 250 μm.

wild-type mean orientations were 87.4° and 93.0°, respectively. Statistical analysis proved the difference to be significant ($p < 0.01$). At 7 DAG, *tor1* and wild-type mean orientations were 66.2° and 92.9°, respectively; the difference was statistically significant ($p < 0.0001$). It was concluded that MTs of *tor1* cortical arrays are disoriented relative to the wild-type control and that, by 7 DAG, MTs with left-handed positions strongly outweigh MTs with right-handed or transverse orientations. The fact that a MT phenotype—the narrowed MT distribution and a slight but distinct left-handed shift—can be detected at 4 DAG when *tor1* hypocotyls have not begun twisting suggests that the MT reorientation is not a side effect of twisted growth and that MTs might have a more causal role in expression of the helical phenotype. In this case, the left-handed offset in the MTs of *tor1* hypocotyls at 4 DAG could be the precursor of the more steeply pitched left-handed helices evident at 7 DAG.

The relationship between MTs and the direction of cell growth is usually explained by assuming that MTs act as templates for the deposition of the load-bearing cellulose microfibrils of the cell wall, with cells elongating perpendicularly to transversely wound cellulose. A recent study [3] has used this model to explain helical growth in *spiral* mutants (however, the exact role of MTs in cellulose deposition is currently under debate; see [12] and [13] for opposite views). According to Furutani et al. [3], expansion perpendicular to cellulose laid down in left-handed helices would result in right-handed growth, and vice versa. Another explanation is that a helix "unwinds" in the opposite direction as it is stretched so that a wall laid down with a left-handed helical pitch would unwind with a right-handed twist as the cell elongates [14].

To investigate the *TOR1* gene further, we identified the *TOR1* locus by fine mapping and complementation. *TOR1* was previously assigned to a central region of chromosome 4 [3, 15]. We applied published markers (PG11, pCITd76) and additional PCR-based markers (Experimental Procedures) to locate *TOR1* to a 111 kb region covered by the BAC clones T24A18 and F21F11 (Figure 2A). Restriction fragments of partially HindIII-digested BAC clones were subcloned into the cosmid vector pBIC20 [16]. After transformation of several overlapping cosmids, three cosmids were found to complement the *tor1* mutation (Figure 2B). Together with overlapping noncomplementing cosmids, these experi-

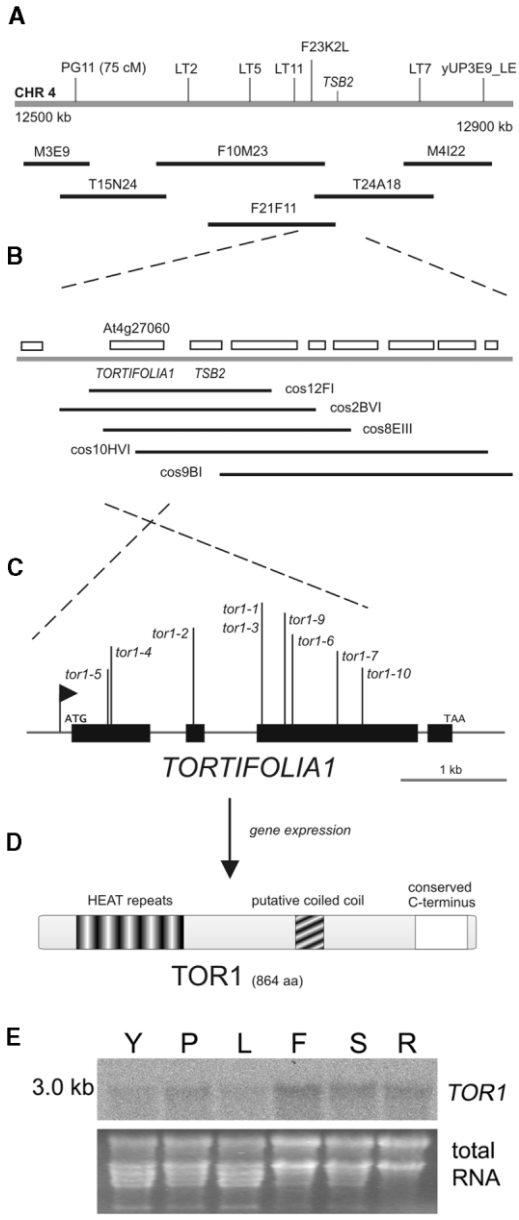

Figure 2. Identification of *TOR1* and Expression from the *TOR1* Gene

(A) *TOR1* was identified by a map-based approach. Genetic markers (indicated on the chromosome) were applied for screening a *tor1* F2 population. Several BAC clones cover the *TOR1* region.

(B) Enlargement from the 111 kb region containing *TOR1*. Annotated genes [18] are indicated by open boxes. Three cosmids (cos2BVI, cos12FI, cos8EIII) complemented the *tor1* phenotype to wild-type in contrast to e.g., cos10HVI and cos9BI. This indicated that the gene At4g27060 next to *TSB2* (tryptophan synthase beta2) codes for *TOR1*.

(C) Structure of the *TOR1* gene and mutant alleles. 5′ RACE defined the start of transcription from *TOR1* gene indicated by a flag. In comparison to the genome annotation, the deduced TOR1 protein carries a 38 amino acid N-terminal extension. The positions of nine *tor1* mutations are indicated (Table S1). The *TOR1* gene has been deposited in GenBank (AJ249836).

(D) Features of the predicted TOR1 protein. The 94 kDa TOR1 protein exhibits five consecutive HEAT repeats in its N-terminal domain. The middle part of the *TOR1* protein contains a putative coiled coil region. An acidic C-terminal domain is conserved among *TOR1* closest homologs.

(E) Northern analysis of *TOR1* expression. Total RNA (20 μg per lane) was separated by gel electrophoresis and blotted onto a nylon membrane. Hybridization with a labeled *TOR1* fragment detected a transcript of 3 kb. Loading was controlled by ethidium bromide staining of the blotted gel. Abbreviations are as follows: Y, young leaf; P, petiole; L, adult leaf; F, inflorescence; S, stem; and R, root.

ments indicated that a single gene, At4g27060, codes for *TOR1* [17]. Sequencing of At4g27060 from *tor1* alleles revealed mutations leading to premature termination of the predicted protein and/or disruption of the *TOR1* open reading frame (Table S1 and Figure 2C), suggesting that helical growth in *tor1* results from the absence of a functional TOR1 protein (*loss of function*).

Sequencing the *TOR1* cDNA (Experimental Procedures) confirmed the splice site predictions for At4g27060 [18]. However, 5′ RACE defined the actual 5′ end of the *TOR1* message to be 193 nucleotides upstream of the annotated translational start. When compared to the annotated gene, the deduced protein shows an N-terminal extension of 38 amino acids; the 5′ untranslated leader has a length of 79 bp (Figures 2C and 2D). Northern experiments revealed a single message of 3.0 kb. The *TOR1* message was detected in all organs examined, including roots, stems, inflorescences, petioles, and leaves. When compared to ubiquitin as an internal standard, *TOR1* gene expression appeared to be low and uniform (data not shown), with slightly stronger expression in the inflorescence (Figure 2E).

The predicted TOR1 protein is 864 amino acids in length, with a molecular mass of 94.0 kDa and a pI of 5.47. BLAST searches against nonredundant GenBank entries revealed that TOR1 has high homology (51% identical amino acids) to the potato HIP2 protein, which was reported to bind to the helper-component proteinase from potyvirus [19]. No function was assigned to the HIP2 protein. Our BLAST searches indicated TOR1 homologs exclusively in the plant kingdom (e.g., in monocotyledonous plants such as rice and in the moss *Physcomitrella patens*). In *Arabidopsis*, TOR1 constitutes a novel family of six conceptual *Arabidopsis* proteins relating to the genes At1g50890, At2g07170, At1g27210, At1g59850, At5g62580, and At4g27060 (Figure 3). The closest *Arabidopsis* homolog of TOR1, AAG50927 from At1g50890, shows 50% identical amino acids.

Homology searches with the TOR1 sequence via the standard BLAST algorithm revealed no significant homology to proteins of known function, but PSI-BLAST searches [20] indicated a distant but obvious homology to HEAT repeat-containing proteins, such as *Tor1* and *Tor2* (target of rapamycin) from yeast, importin-β, and protein phosphatase 2A. HEAT repeat domains are capable of mediating protein-protein interactions. A similarity of TOR1 with HEAT repeat proteins was supported by the IMPALA block-searcher algorithm [21]. TOR1 sequence comparisons based on hidden Markov models [22] yielded best results for proteins with HEAT, but also for proteins with ARM repeats. HEAT repeats and the evolutionarily related ARM repeats can be detected by

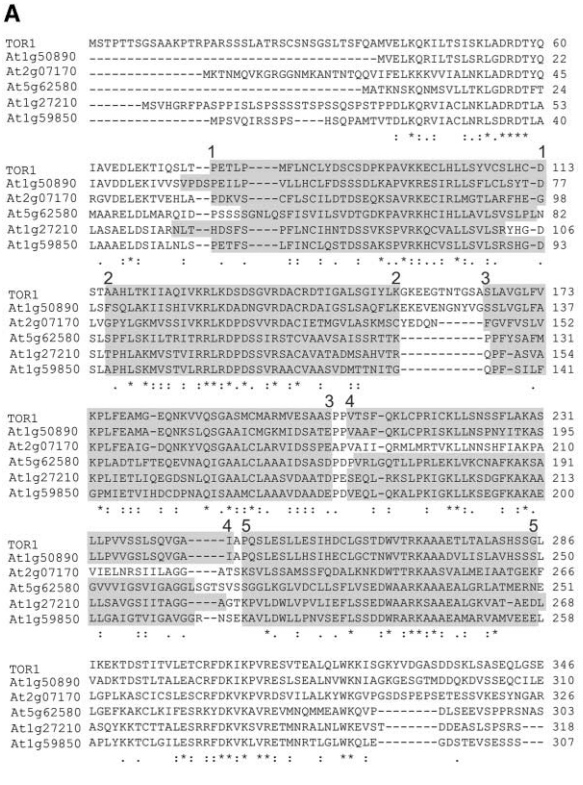

Figure 3. The TOR1 Family of TOR1-like Proteins in *Arabidopsis*; Partial Sequence Alignment

(A) N-terminal conserved region of TOR1-like proteins. The predicted HEAT repeats are numbered and shaded gray. At2g07170 lacks the fourth HEAT repeat.

(B) The putative coiled-coil region is enclosed by the box, and the four amino acids of the hypothetical stutter are shaded gray. The predicted coiled-coil heptad pattern [25] is assigned by the amino acid positions (a) and (d). Sequence comparison was performed with Clustal W [40]. An asterisk indicates identical amino acids, a colon indicates a conservative amino acid exchange, and a period indicates semi-conservative amino acid exchange.

the REP search algorithm [23]. Sequences from individual TOR1 family members do not yield above-threshold values when they are analyzed with this program. However, significant matches were obtained after consensus sequences (generated by BlockMaker [24]) from the TOR1 family were applied to the REP search algorithm. Comparing the REP outputs for consensus sequences with the output for the simple TOR1 sequence enabled us to detect at least five consecutive HEAT repeats in the TOR1 N-terminal region. We used the same method to detect HEAT repeats in the other TOR1 family members (Figure 3A).

Two other regions of elevated conservation are found in the TOR1 protein as compared to the *Arabidopsis* family members (Figures 2D and 3B). One of these, the central conserved region of TOR1, is predicted to form a coiled-coil structure according to the COILS program [25]. The MultiCoil program [26] verified this for the closer homologs of TOR1 (proteins from At1g50890 and At2g07170). The predicted coiled-coil region in TOR1 spans the amino acids 510–560 and appears to contain a single stutter [27].

To determine the subcellular localization of the TOR1 protein, we synthesized a full-length *TOR1* cDNA by RT-PCR, coupled it to *GFP*, and used it to transform plants and suspension cells (Experimental Procedures). TOR1-GFP labels cortical MTs in epidermal cells of transgenic *Arabidopsis* seedlings (Figure 4A). To establish that TOR1-GFP is a functional protein, we demonstrated that its CaMV 35S-driven expression complements homozygous *tor1* plants (Figures 4B and 4C). In order to study the distribution of TOR1-GFP during the cell cycle, we transformed tobacco BY-2 suspension cells. TOR1-GFP labels the four-plant MT arrays (Figures 4D–4G). However, because only the decoration of the cortical MTs (Figures 4A and 4D) is relevant to the *tor1* phenotype, which is expressed during the elongation phase of G1, it is not clear that these other labeling patterns are indicative of a function for TOR1 during cell division.

In principle, decoration of cortical microtubules by TOR1-GFP in vivo could be direct or indirect via another protein. To address this question, we expressed TOR1-His in a yeast expression system and performed pull-downs with taxol-stabilized MTs over a sucrose cushion. Figure 4H shows that the approximately 95 kDa TOR1-His protein copurified with MTs (lane 3). In controls, TOR1-His did not precipitate by itself in the absence of MTs. A dummy His-tagged protein, UDP-glucose transferase (At4g15550), also did not pellet with MTs (data not shown). This confirms that TOR1 directly binds MTs, which together with the in vivo localization indicates that TOR1 can be classified as a microtubule-associated protein. SPR1/SKU6, a protein revealed by another helical-growth mutant, also decorates cortical MTs as a GFP fusion gene, but it does not bind to MTs in vitro, implying that it is not a microtubule-associated protein (MAP) and must bind via another protein [28, 29]. However, the additive phenotype of the double *spr1/tor1* mutant [3] does not provide positive evidence for a possible interaction between SPR1 and TOR1.

Other recently discovered plant MAPs have been found to be related to those in other eukaryotes; MAP65 is related to PRC1 of metazoa (and yeast Ase1p, [30]), whereas MOR1 is related to the ch-TOG/XMAP215 family [31, 32]. However, simple BLAST searches with the TOR1 sequence do not reveal significant matches with proteins of known function. All obvious TOR1 homologs are plant sequences; the nearest hypothetical, non-plant relative was found in *Dictyostelium discoideum* (AA050914) but had a BLAST E-value of only $1e^{-04}$. It would therefore appear that TOR1 is a plant-specific microtubule-associated protein, which is consistent with its role in regulating the plant cell's characteristic cortical MT array. TOR1, in the wild-type, is evidently responsible for maintaining straight growth, which in the hypocotyls is associated with a mixture of left- and right-handed MT helices. In the mutant, left-handed MT arrays predominate, and so the function of TOR1 would seem to suppress

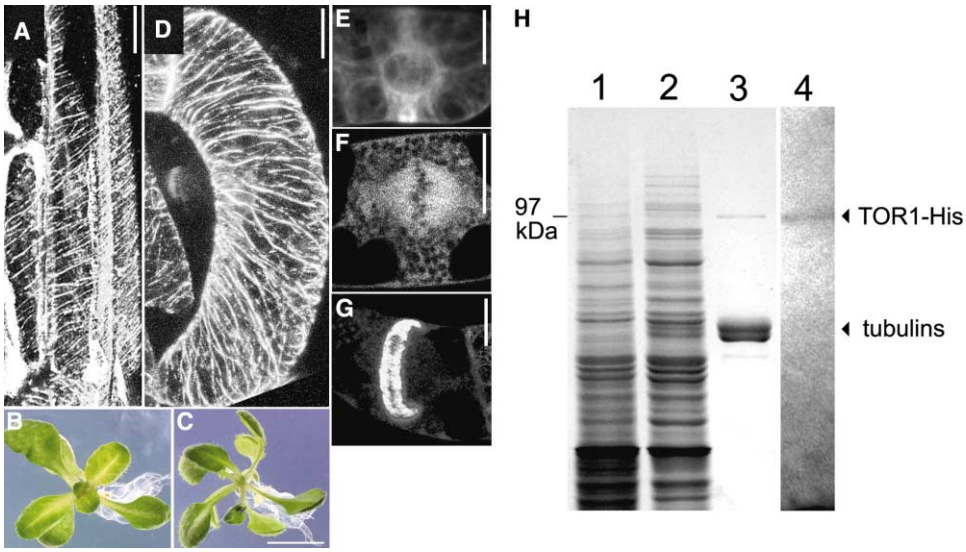

Figure 4. Recombinant TOR1 Binds MTs In Vivo and In Vitro

(A) TOR1-GFP expression in epidermal cells of *Arabidopsis* seedlings labels cortical MT.

(B) The TOR1-GFP fusion has wild-type function, as indicated by complementation of the helical-growth defect in a *tor1* background.

(C) Helical growth of a *tor1* plant.

(D–G) TOR1-GFP labels MTs in tobacco BY-2 suspension cells. (D) Interphase cortical MT array. (E) Preprophase band. (F) Metaphase spindle. (G) Phragmoplast.

(H) TOR1-His binds to microtubules in vitro. Lane 1, Coomassie-stained gel of protein extract from yeast expressing TOR1-His without added MTs; lane 2, supernatant after addition of taxol-MTs; lane 3, MT pellet with precipitated TOR1-His; lane 4, MT pellet after blotting and specific detection of the His-epitope in TOR1-His. Scale bars in (A) and (D)–(G) represent 20 μm, and those in (B) and (C) represent 5 mm.

this tendency and to allow the formation of right-handed arrays. Other factors that impact upon MTs also induce helical growth. For example, *microtubule organization1* (*mor1*) mutations, the MT-stabilizing plant metabolite taxol, and the destabilizing herbicide, propyzamide, can all phenocopy the helical-growth patterns [3, 31]. A common thread among these diverse agents is their potential for affecting MT stability and turnover, and so it is possible that TOR1 controls the direction of growth via an effect on MT dynamics, although how this is translated into information on the helical sign is an open question.

In conclusion, our results show that TOR1 is a cytoskeletal protein found in plants and has no obvious homologs in the animal kingdom. In *tor1* mutants, the right-handed twisting of the hypocotyl is preceded by a shift in cortical microtubule orientation. Recombinant TOR1 proteins bind microtubules in vivo and in vitro. These results indicate that TOR1 is a novel cytoskeletal player required for wild-type cortical microtubule orientation. TOR1 functions as a microtubule-associated protein whose mutation results in a switch from straight growth to a twisted phenotype.

Experimental Procedures

Mutant Strains

Mutants displaying the *tortifolia* phenotype were identified in an ethane methylsulfonate-mutagenized Landsberg *erecta* population; additional alleles were obtained from other researchers (Table S1). For allelism tests (mutants *tor1-1* to *tor1-8*) mutants were crossed, and segregation of phenotypes was followed up to the F2 generation. These *tor1* mutations are inherited as recessive traits. Insertional mutants of At4g27060 (*TOR1*) identified in the SALK collection [33] showed *tortifolia* phenotypes; DNA sequencing confirmed insertion into the *TOR1* gene (Table S1). No allelic series was observed for *tor1* alleles 1–9; in contrast, *tor1-10* shows less strong petiole twisting. *tor1-1* (N378) and *tor1-5* (N258) are available from the Nottingham *Arabidopsis* Stock Center.

Mapping and Identification of *TOR1*

The method of analyzing DNA duplices on high-resolution gels [34] allowed the identification of several polymorphisms in the *TOR1* region on chromosome 4 (markers LT2, LT7, LT11, and F23K2L). Markers LT5 and 3E9_LE are of SSLP and CAPS types, respectively. Screening of 1600 *tor1* progenies from crossings between *tor1-1* and L*er* indicated that *TOR1* localizes between the markers LT5 and LT7. For locating *TOR1* within this region, 12 to 22 kb fragments from partially HindIII-digested BAC-DNA (T24A18 and F21F11) were cloned into the pBIC20 cosmid vector [16]. Cosmids propagated in *E. coli* NM554 were analyzed by PCR markers and restriction digests. A contig of overlapping cosmids spanning the *TOR1* region was established. After electroporation into *Agrobacterium tumefaciens* (pGV3101/pMP90), cosmids were transformed into *tor1* plants via floral dip [35]. Transgenic plants were selected on agar plates containing 50 μg/ml kanamycin. Confirmation of complete T-DNA transfer was achieved by GUS staining [16]. T2 plants were analyzed for segregation of wild-type and *tor1* phenotypes.

Northern Analysis and 5′ RACE

For Northern analysis [36], 20 μg total RNA per lane were separated on 1% agarose gels containing formaldehyde and transferred to a nylon membrane (Amersham). A *TOR1*-specific probe was generated by PCR with 5′-TCTCTCACCAGACTCTGCTTC-3′ and 5′-TCCAGATGCTTTATTATCCCACC-3′. After random primed labeling with [^{33}P]dATP, hybridizations were carried out with formamide. Signals were detected with the FLA-3000 phosphoimager (Fuji).

For analysis of the *TOR1* 5′ end by 5′ RACE, the *TOR1*-specific oligonucleotide 5′-AAAGCTTTTGGAAAGAAGTAACTGG-3′ was used for priming the reverse transcriptase reaction (Gibco BRL). Two rounds of nested PCRs were performed. The 5′ *TOR1* fragments

obtained were cloned. The DNA sequence of nine independent clones pointed to the same transcriptional start of *TOR1*.

Recombinant Expression of *TOR1*

A full-length *TOR1* cDNA was synthesized from *Arabidopsis* Columbia RNA by RT-PCR with 5′-GAGAGCGGTCGACGTCGGAGATTTA GAAATGAGCAC-3′ and 5′-CTGTCTGGTCGACAATTATGAACAACA ACGGTACTGAAG-3′ and cloned into a pUC19 derivative. This construct served for downstream cloning reactions. The ORF of *TOR1* was PCR amplified without a stop codon via GATEWAY adaptor oligonucleotides and recombined into pDONR221 (Invitrogen). Subsequently, *TOR1* was recombined into pK7FWG2 [37] to allow expression of a fusion with GFP linked to the C terminus of TOR1 under the control of CaMV 35S promoter. *Arabidopsis* plants were transformed with *Agrobacterium* by floral dip. Tobacco BY-2 cells were transformed by coincubation with *Agrobacterium* for 2 days, followed by several washes with BY2-medium and selection on agar plates containing kanamycin (200 μg/ml), carbencillin (500 μg/ml), and rovral (20 μg/ml). For expression of TOR1-His in yeast (strain INVSc1), the *TOR1* cDNA was excised from the pUC19 derivate and ligated into pYES2 (Invitrogen). An oligonucleotide encoding six His residues was attached to the *TOR1* 3′ end by PCR cloning. The fusion protein was expressed by galactose-induction and extracted by the glass-bead method (pYES2 manual, Invitrogen).

MT Cosedimentation

TOR1-His was pelleted from protein preparations supplemented with 10 mM EGTA (final concentration) and 20 μM taxol (final concentration; Sigma) through a 40% (w/v) sucrose cushion with taxol-stabilized MTs (final concentration 0.5 mg/ml bovine tubulin; Cytoskeleton) as described by Chan et al. [38]. For identification of His-tagged proteins after Western transfer, blots were probed with the INDIA HisProbe-HRP (Pierce).

Immunolabeling of MTs from *Arabidopsis* Hypocotyl Epidermal Cells and Quantification

Wild-type (Enkheim) and *tor1-1* were grown on soil with a 16/8 hr day/night cycle. Seedlings were picked with tweezers, and the roots were cut off. Fixation and opening of the tissue were performed as described by Wasteneys et al. [39]. MT labeling was achieved with monoclonal anti-α-tubulin (T 9026, Sigma) and Alexa Fluor 488 goat anti-mouse IgG (A-11001, Molecular Probes). After labeling, tissues were mounted in Vectashield (H-1000, Vector Laboratories) and analyzed with a confocal microscope (Zeiss LSM 510). Projections of Z scans (AIM software, versus 3.0; Carl Zeiss Jena) converted to JPEG format (with Adobe Photoshop 7.0) were used for measuring the angle of MTs with respect to the cell's longitudinal axis via the ImageJ 1.30t program (Wayne Rasband, National Institutes of Health). Only MTs from outer tangential walls of epidermal cells were used for quantification. All cells taken for measurement were from the upper half of the hypocotyl, i.e., ≤ 700 μm (4 DAG) and ≤ 1450 μm (7 DAG) below the petiole junction. MTs in an array generally shared the same direction. However, for estimation of the mean orientation of a given cortical array, a line was drawn down the cell, and the angle of MTs was measured at eight regular points for 4 DAG seedlings. For the longer cells in 7 DAG seedlings, 12 points were taken. MT angles were measured at >750 points from >125 cells for both wild-type and *tor1* at 4 DAG stage and at >620 points from >100 cells for both wild-type and *tor1* at 7 DAG stage. Statistical analysis of MT orientations was performed with both nonparametric and parametric tests (Rank Sum test and t test, respectively) with the SAS package (SAS Institute Inc.). The p values given in the text relate to the output of both tests.

Supplemental Data

One supplemental table and one supplemental figure are available with this article online at http://www.current-biology.com/cgi/content/full/14/16/1515/DC1/.

Acknowledgments

We are indebted to R.A. Torres-Ruiz, J. Sheen, and B. Steipe for valuable discussions and to R. Schmidt for contributing information on molecular markers. We thank T. Hashimoto for exchanging *spr2* mutant seeds prior to publication. This work was supported by the Deutsche Forschungsgemeinschaft (DFG Scha 454/5), by Fonds der Chemischen Industrie, and by a Biotechnology and Biological Sciences Research Council grant to C.W.L.

References

1. Yuen, C.Y., Pearlman, R.S., Silo-Suh, L., Hilson, P., Carroll, K.L., and Masson, P.H. (2003). WVD2 and WDL1 modulate helical organ growth and anisotropic cell expansion in Arabidopsis. Plant Physiol. *131*, 493–506.
2. Thitamadee, S., Tuchihara, K., and Hashimoto, T. (2002). Microtubule basis for left-handed helical growth in Arabidopsis. Nature *417*, 193–196.
3. Furutani, I., Watanabe, Y., Prieto, R., Masukawa, M., Suzuki, K., Naoi, K., Thitamadee, S., Shikanai, T., and Hashimoto, T. (2000). The SPIRAL genes are required for directional control of cell elongation in Aarabidopsis thaliana. Development *127*, 4443–4453.
4. Wasteneys, G.O. (2000). The cytoskeleton and growth polarity. Curr. Opin. Plant Biol. *3*, 503–511.
5. Bürger, D. (1971). Die morphologischen Mutanten des Göttinger Arabidopsis-Sortiments, einschließlich der Mutanten mit abweichender Samenfarbe. Arab. Inf. Serv. *8*, 36–42.
6. Gendreau, E., Traas, J., Desnos, T., Grandjean, O., Caboche, M., and Hofte, H. (1997). Cellular basis of hypocotyl growth in Arabidopsis thaliana. Plant Physiol. *114*, 295–305.
7. Takesue, K., and Shibaoka, H. (1998). The cyclic reorientation of cortical microtubules in epidermal cells of azuki bean epicotyls: the role of actin filaments in the progression of the cycle. Planta *205*, 539–546.
8. Yuan, M., Warn, R.M., Shaw, P.J., and Lloyd, C.W. (1995). Dynamic microtubules under the radial and outer tangential walls of microinjected pea epidermal cells observed by computer reconstruction. Plant J. *7*, 17–23.
9. Flanders, D.J., Rawlins, D.J., Shaw, P.J., and Lloyd, C.W. (1989). Computer-aided 3-D reconstruction of interphase microtubules in epidermal cells of Datura stramonium reveals principles of array assembly. Development *106*, 531–541.
10. Liang, B.M., Dennings, A.M., Sharp, R.E., and Baskin, T.I. (1996). Consistent handedness of microtubule arrays in maize and Arabidopsis primary roots. Protoplasma *190*, 8–15.
11. Sugimoto, K., Williamson, R.E., and Wasteneys, G.O. (2000). New techniques enable comparative analysis of microtubule orientation, wall texture, and growth rate in intact roots of Arabidopsis. Plant Physiol. *124*, 1493–1506.
12. Burk, D.H., and Ye, Z.H. (2002). Alteration of oriented deposition of cellulose microfibrils by mutation of a katanin-like microtubule-severing protein. Plant Cell *14*, 2145–2160.
13. Sugimoto, K., Himmelspach, R., Williamson, R.E., and Wasteneys, G.O. (2003). Mutation or drug-dependent microtubule disruption causes radial swelling without altering parallel cellulose microfibril deposition in Arabidopsis root cells. Plant Cell *15*, 1414–1429.
14. Lloyd, C., and Chan, J. (2002). Helical microtubule arrays and spiral growth. Plant Cell *14*, 2319–2324.
15. Fabri, C.O., and Schäffner, A.R. (1994). An Arabidopsis thaliana RFLP mapping set to localize mutations to chromosome regions. Plant J. *5*, 149–156.
16. Meyer, K., Leube, M.P., and Grill, E. (1994). A protein phosphatase 2C involved in ABA signal transduction in Arabidopsis thaliana. Science *264*, 1452–1455.
17. Buschmann, H. (2002). TORTIFOLIA Gene kontrollieren das Streckungswachstum in Arabidopsis. Klonierung von TORTIFOLIA1. PhD Thesis, University of Munich LMU, Munich, Germany.
18. The Arabidopsis Genome Initiative. (2000). Analysis of the genome sequence of the flowering plant Arabidopsis thaliana. Nature *408*, 796–815.
19. Guo, D., Spetz, C., Saarma, M., and Valkonen, J.P. (2003). Two potato proteins, including a novel RING finger protein (HIP1), interact with the potyviral multifunctional protein HCpro. Mol. Plant Microbe Interact. *16*, 405–410.

20. Altschul, S.F., Madden, T.L., Schaffer, A.A., Zhang, J., Zhang, Z., Miller, W., and Lipman, D.J. (1997). Gapped BLAST and PSI-BLAST: a new generation of protein database search programs. Nucleic Acids Res. *25*, 3389–3402.
21. Schaffer, A.A., Wolf, Y.I., Ponting, C.P., Koonin, E.V., Aravind, L., and Altschul, S.F. (1999). IMPALA: matching a protein sequence against a collection of PSI-BLAST-constructed position-specific score matrices. Bioinformatics *15*, 1000–1011.
22. Karplus, K., Barrett, C., and Hughey, R. (1998). Hidden Markov models for detecting remote protein homologies. Bioinformatics *14*, 846–856.
23. Andrade, M.A., Ponting, C., Gibson, T., and Bork, P. (2000). Homology-based method for identification of protein repeats using statistical significance estimates. J. Mol. Biol. *298*, 521–537.
24. Henikoff, S. (1995). Comparative methods for identifying functional domains in protein sequences. Biotechnol. Annu. Rev. *1*, 129–147.
25. Lupas, A. (1996). Coiled coils: new structures and new functions. Trends Biochem. Sci. *21*, 375–382.
26. Wolf, E., Kim, P.S., and Berger, B. (1997). MultiCoil: a program for predicting two- and three-stranded coiled coils. Protein Sci. *6*, 1179–1189.
27. Brown, J.H., Cohen, C., and Parry, D.A. (1996). Heptad breaks in alpha-helical coiled coils: stutters and stammers. Proteins *26*, 134–145.
28. Sedbrook, J.C., Ehrhardt, D.W., Fisher, S.E., Scheible, W.R., and Somerville, C.R. (2004). The Arabidopsis SKU6/SPIRAL1 gene encodes a plus end-localized microtubule-interacting protein involved in directional cell expansion. Plant Cell *16*, 1506–1520.
29. Nakajima, K., Furutani, I., Tachimoto, H., Matsubara, H., and Hashimoto, T. (2004). SPIRAL1 encodes a plant-specific microtubule-localized protein required for directional control of rapidly expanding Arabidopsis cells. Plant Cell *16*, 1178–1190.
30. Schuyler, S.C., Liu, J.Y., and Pellman, D. (2003). The molecular function of Ase1p: evidence for a MAP-dependent midzone-specific spindle matrix. Microtubule-associated proteins. J. Cell Biol. *160*, 517–528.
31. Whittington, A.T., Vugrek, O., Wei, K.J., Hasenbein, N.G., Sugimoto, K., Rashbrooke, M.C., and Wasteneys, G.O. (2001). MOR1 is essential for organizing cortical microtubules in plants. Nature *411*, 610–613.
32. Hussey, P.J., and Hawkins, T.J. (2001). Plant microtubule-associated proteins: the HEAT is off in temperature-sensitive mor1. Trends Plant Sci. *6*, 389–392.
33. Alonso, J.M., Stepanova, A.N., Leisse, T.J., Kim, C.J., Chen, H., Shinn, P., Stevenson, D.K., Zimmerman, J., Barajas, P., Cheuk, R., et al. (2003). Genome-wide insertional mutagenesis of Arabidopsis thaliana. Science *301*, 653–657.
34. Hauser, M.T., Adhami, F., Dorner, M., Fuchs, E., and Glossl, J. (1998). Generation of co-dominant PCR-based markers by duplex analysis on high resolution gels. Plant J. *16*, 117–125.
35. Clough, S.J., and Bent, A.F. (1998). Floral dip: a simplified method for Agrobacterium-mediated transformation of Arabidopsis thaliana. Plant J. *16*, 735–743.
36. Ausubel, F.M., Brent, R., Kingston, R.E., Moore, D.D., Seidman, J.G., Smith, J.A., and Struhl, K. (1987). Current Protocols in Molecular Biology. (New York, NY.: John Wiley).
37. Karimi, M., Inze, D., and Depicker, A. (2002). GATEWAY vectors for Agrobacterium-mediated plant transformation. Trends Plant Sci. *7*, 193–195.
38. Chan, J., Rutten, T., and Lloyd, C. (1996). Isolation of microtubule-associated proteins from carrot cytoskeletons: a 120 kDa map decorates all four microtubule arrays and the nucleus. Plant J. *10*, 251–259.
39. Wasteneys, G.O., Willingale-Theune, J., and Menzel, D. (1997). Freeze shattering: a simple and effective method for permeabilizing higher plant cell walls. J. Microsc. *188*, 51–61.
40. Thompson, J.D., Higgins, D.G., and Gibson, T.J. (1994). CLUSTAL W: improving the sensitivity of progressive multiple sequence alignment through sequence weighting, position-specific gap penalties and weight matrix choice. Nucleic Acids Res. *22*, 4673–4680.

Accession Numbers

The *TOR1* gene has been deposited at the EMBL database (AJ249836).

Note Added in Proof

While this manuscript was in press, Shoji et al. from T. Hashimoto's laboratory submitted for publication an independent analysis of *SPR2*, which is allelic to *TOR1*.